SAND2004-3114
Printed June 2004

Solderability Study of 63Sn-37Pb on Zinc-Plated and Cadmium-Plated Stainless Steel For The MC4636 Lightning Arrestor Connector

Edwin P. Lopez, Corrosion, and Surface Sciences,
Dr. Paul T. Vianco, Jerome A. Rejent, and Joe Martin, Materials Reliability

Sandia National Laboratories[1]
Albuquerque, NM

Abstract

Cadmium plating on metal surfaces is commonly used for corrosion protection and to achieve good solderability on the 304L stainless steel shell of the MC4636 lightning arrestor connector (LAC) for the W76-1 system. This study examined the use of zinc as a potential substitute for the cadmium protective surface finish. Tests were performed with an R and RMA flux and test temperatures of 230ºC, 245ºC, and 260ºC. Contact angle, θ_C, served as the generalized solderability metric. The wetting rate and wetting time parameters were also collected. The solderability (θ_C) of the Erie Plating Cd/Ni coatings was better than that of similar Amphenol coatings. Although the θ_C data indicated that both Cd/Ni platings would provide adequate solderability, the wetting rate and wetting time data showed the Amphenol coatings to have better performance. The Zn/Ni coatings exhibited non-wetting under all flux and temperature conditions. Based on the results of these tests, it has been demonstrated that zinc plating is not a viable alternate to cadmium plating for the LAC connectors

[1]Sandia is a multiprogram laboratory operated by Sandia Corporation, a Lockheed Martin Company, for the United States Dept. of Energy's National Nuclear Security Administration under Contract DE-AC04-94AL85000.

Acknowledgements

The authors greatly appreciate the analytical work of Richard P. Grant and Michael J. Rye of Sandia National Laboratories. Mike Hosking graciously reviewed the manuscript.

Contents

Table

Figure

1. INTRODUCTION

Carcinogenic risks associated with the use of cadmium (Cd) as a plating material have led to the consideration of zinc (Zn) as an alternative coating. Cadmium over nickel (Ni) has been a standard plating method on 304L stainless steel in order to provide both corrosion protection and good solderability for next assembly operations. The purpose of the Ni coating is to provide a solderable layer for next assembly processes. The Cd coating serves as the protective surface finish, preserving the solderability of the Ni layer surface. Because of these attributes, Cd/Ni coatings have been specified for the MC4636 Lightning Arrestor Connector on the W76 system. The present study examined the solderability of 63Sn-37Pb (wt.%) on Zn/Ni-plated and Cd/Ni-plated 304L stainless steel as a function of solder flux and temperature. The solder fluxes were a rosin-based material (R) and a rosin-based mildly activated (RMA) composition. The solderability tests were performed at three different test temperatures: 230ºC, 245ºC, and 260ºC.

The solderability metric was the contact angle, θ_C, formed when a substrate coupon is immersed edge-on into molten solder.[1] The contact angle is determined by the equilibrium balance of the three interfacial tensions, as expressed by Young's equation:

$$\gamma_{SF} - \gamma_{SL} = \gamma_{LF} \cos\theta_C \qquad \text{Equation 1}$$

where γ_{SF} is the solid (substrate)-flux interfacial tension; γ_{SL} is the solid-liquid (solder) interfacial tension, and the γ_{LF} is the liquid-flux interfacial tension (Figure 1). The smaller the value of θ_C, the better the solderability performance. The value of θ_C is minimized when γ_{LF} is minimized, γ_{SF} is maximized and γ_{SL} is minimized.

The meniscometer/wetting balance test was used to determine the value of θ_C.[2] The measurements are illustrated in Figure 2. The meniscometer test was used to measure the maximum meniscus rise or height (H) of molten solder on the face of a coupon test sample immersed edge-on into the solder bath. The wetting balance test was used to determine the weight of the solder meniscus as a function of time. Shown in Figure 3 is a generalized representation of the plot of meniscus weight as a function of test time. When a coupon is initially immersed into the solder bath, an "upwards" force is exerted on the sample. This force has two contributions, (1) the solder displaced by the sample volume and (2) the solder displaced by the action of the surface tension, that is, the "negative" meniscus. As wetting takes place, the negative meniscus decreases and the solder wets/spreads up the sample surface, creating a downward force due to its weight. The buoyancy force due to solder displaced by the submerged volume of the coupon remains the same and must be accounted for in the meniscus weight calculations by subtracting its fixed value from the total measured force. The maximum meniscus weight, W, is used in the calculation of θ_C.

The value of θ_C was calculated from H and W, using equation (2):

$$\theta_c = \sin^{-1}\left[\frac{4w^2 - \left(\rho g P H^2\right)^2}{4w^2 + \left(\rho g P H^2\right)^2}\right] \qquad \text{Equation 2}$$

where ρ is the solder density (gm/cm^3), g is the acceleration due to gravity (cm/sec^2), and P is the sample perimeter (cm). The solder flux interfacial tension, γ_{LF}, can also be independently determined from the experimental data using equation (3):

$$\gamma_{LF} = \frac{\rho g}{4}\left\{\frac{4w^2}{(\rho g P H)^2} + H^2\right\} \qquad \text{Equation 3}$$

In addition to the parameter, W, the wetting balance curve is used to identify the wetting rate and time to maximum wetting force parameters, which are also depicted in Figure 3.

The meniscometer/wetting balance tests were performed with 63Sn-37Pb on Cd/Ni and Zn/Ni-plated 304L stainless steel coupons. The objective of these evaluations was to determine the solderability of Zn/Ni coatings on stainless steel substrates. The performance of the Zn/Ni finish was compared to that of the Cd/Ni finish that is currently used in the MC4636 LAC in order to determine the suitability of the former on this component.

2. EXPERIMENTAL PROCEDURES

2.1 Substrate Preparation

The 304L stainless steel substrates had nominal dimensions of 2.54 x 2.54 x 0.0254 cm. The coupons were sheared from rolled sheet stock and flattened to remove any residual curvature. Only those coupons were used that had length and width dimensions to within ±0.013 cm of their nominal values. Amphenol Plating Company and Erie Plating Company provided the electroplating services. The electroplated Ni layer had a Ni-P composition (0.0026 to 0.0038 wt.% P). The Cd/Ni-plated coupons that were prepared by Amphenol had a 5.5 μm-thick Ni solderable layer and a 10 μm-thick Cd protective layer. These thicknesses were determined by Scanning Electron Microscopy (SEM), as shown by Figure 4. The coupons prepared at Amphenol were plated in a caustic/cyanide solution having the following nominal concentrations: (1) 2 ounces/gallon cadmium, (2) 17 ounces/gallon cyanide, (3) 3 ounces/gallon caustic

(NaOH), at a temperature of 70 ºF with a cathode current density of 15 amps per square foot. Cadmium-plated samples prepared by Erie had a 0.5 μm-thick Ni solderable layer and 10 μm-thick Cd protective layer as determined by SEM (Figure 5). The Zn/Ni-plated samples that were prepared by Erie Plating had a 0.5 μm thick Ni solderable layer and an 8.6 μm-thick Zn protective layer, as shown in Figure 6. Note that the Amphenol plated nickel layer was much thicker than the nickel layer provided by the Erie Plating Company (5.5 μm versus 0.5 μm). Erie Plating Company did not provide specific Zn/Ni plating bath information. Amphenol did not prepare Zn/Ni-plated samples. Prior to processing, each coupon was degreased using trichloroethylene and isopropyl alcohol (IPOH) and then immediately coated with a flux.

2.2 Solders and Fluxes

All coupons were tested using the eutectic 63Sn-37Pb (wt.%) solder that has a melting temperature of 183ºC. Solderability tests were performed with the molten solder held at 230ºC, 245ºC, or 260ºC. Two solder fluxes were tested. Their compositions were a rosin-based (R) flux and a rosin-based mildly activated (RMA) flux. The fluxes were diluted one-to-one by volume with IPOH.

2.3 Solderability Testing

The meniscus height, H, was evaluated with a meniscometer. The meniscometer measures the maximum vertical movement of a solder meniscus up the face of the coupon that is immersed edge-on into the molten solder. The test procedure went as follows: (1) The coupon was coated with one of the two fluxes: (2) The flux was allowed to dry for 10 minutes: (3) The coupon was then preheated above the solder pot for 20 seconds before being immersed into the solder pot. The maximum meniscus height, H,

was recorded 20 seconds after the immersion. Five tests were performed per each test condition. A mean value for H, along with one standard deviation was determined from those replicate tests.

During meniscometer testing, a false solder wetting front was formed on all of the Cd-plated coupons, which gave rise to erroneous meniscus height measurements. Energy Dispersive X-ray Spectral Imaging was used to determine the composition and thickness of the reaction area at the solder front of the samples. The three samples (one from Amphenol Plating and two from Erie Plating) that were analyzed indicated that the solder front actually advanced undercutting the Cd layer, as shown in Figure 7. Only one sample showed a Ni, P layer between the 304L SS and the Cd layer. In this sample, the solder front undermined the Ni, P layer and the Cd layer. Because of this phenomenon, the height measurements for each Cd dipped sample were re-evaluated using precision calipers.

The meniscus weight of the solder was measured using the wetting balance test apparatus.[2] Five separate tests were performed with this technique as well. The maximum meniscus weight, W, was determined for each test; these values were combined to determine a mean value and one standard deviation that served as the error term.

The contact angle, θ_C, and solder flux interfacial tension, γ_{LF}, were calculated through the use of equations (2) and (3), respectively. The mean values of θ_C and γ_{LF} were determined by inserting the mean values of H and W into those equations. In the case of 63Sn-37Pb solder, the value of ρ is 8.49 g/cm^2. The parameter g and P were 980 cm/sec^2 and 5.085 cm, respectively. The error terms for θ_C and γ_{LF} were calculated by the

following procedure. The maximum value of W, which equaled the mean plus one standard deviation, and minimum value of H, which equaled the mean minus the standard deviation, were inputed into equations (2) and (3). The resulting θ_C and γ_{LF} values were the maximum. The reverse process was performed to determine the minimum values of θ_C and γ_{LF}. The minima and maxima of θ_C and γ_{LF} provided the error terms for these parameters.

Solderability was quantified by the contact angle, θ_C, formed between the liquid solder and the substrate and calculated from equation (2). A qualitative solderability guideline is depicted in Table 1.[3] Wetting is considered to take place when the contact angle is less than 90º. Preferable solderability is accompanied by contact angles that are generally <30º.

3. Test Results and Discussion

3.1 Contact Angle Test Data: Cd/Ni Plated 304L Stainless Steel Samples

An analysis of the solderability behavior [i.e., θ_C, γ_{LF}, and $(\gamma_{SF}- \gamma_{SL})$] of the Cd/Ni plated substrates began by addressing those samples having the Amphenol coating. The performance of the Erie Plating samples was evaluated next. Lastly, comparative generalizations were developed from these individual analyses of the two plating sources.

With the exception of the R flux and 230ºC test temperature, the remaining flux and temperature test combinations resulted in values of θ_C in the range of 30 – 39º on the Amphenol Cd/Ni plated samples (Table 2 & Figures 8-9). Although the contact angle values were considered to represent "good" solderability, they did not exhibit the expected, systematic dependence upon either the flux strength – the contact angle is reduced by the stronger RMA flux – or test temperature – the contact angle decreases

with higher test temperature. A contributing factor may have been the thicker nickel layer, which would not be completely dissolved by the solder even at the higher test temperature. The limited temperature effect was not unexpected, based upon prior solderability studies. It was interesting that the dependence of γ_{LF} on temperature was not monotonic for either flux, showing a maximum at 245ºC. Both R and RMA fluxes exhibited values of (γ_{SF}- γ_{SL}) that decreased with increasing temperature – more so, this was true of the R flux – suggesting that re-oxidation of the plating surface was responsible for the loss of efficacy at the higher test temperatures.

On the other hand, it was considered unusual that the RMA flux did not provide an improved performance vis-à-vis the R flux. In fact, the mean values of θ_C attributed to the R flux were slightly lower than those associated with the RMA flux. A review of the solder-flux interfacial tension parameter indicated that the values of γ_{LF} were significantly lower for the R flux than for the RMA flux. (It is emphasized that γ_{LF} is an independently calculated parameter.) Although a lower γ_{LF} can give rise to a reduced θ_C value, the magnitudes of the differences in γ_{LF} between the two fluxes were much greater than would be required to cause the small differences in θ_C. Therefore, there was a compensating effect provided by the (γ_{SF}- γ_{SL}) term. The R flux resulted in a value of (γ_{SF}- γ_{SL}) that was smaller relative to that associated with the RMA flux in each case. This trend was expected because the less active R flux has a reduced oxide removal efficacy and, as such, produces a lower γ_{SF} as compared to the performance of the RMA flux. (The value of γ_{SF} remains unchanged because of the similar solderable finish, Ni.) In conclusion, the similarity in the contact angles of 63Sn-37Pb solder on the Amphenol

Cd/Ni plated substrates was a result of the R flux having a lower γ_{LF} value than the RMA flux, which compensated for the former fluxes' lower efficacy (i.e., lower γ_{SF}).

Next, the solderability of the Erie Plating Cd/Ni plated samples was assessed. The contact angle values in Table 2 and plot in Figure 9 indicate an overall solderability performance that ranged from excellent to adequate. Unlike the Amphenol Cd/Ni layer, the contact angle θ_C exhibited the expected tendencies on flux type and test temperature with the Erie Plating layers. First, solderability improved with higher test temperature. In the case of the R flux, non-monotonic changes of both γ_{LF} and (γ_{SF}- γ_{SL}) combined to give rise to the overall trend of improved solderability with higher test temperature. On the other hand, the RMA flux exhibited monotonic decreases of both γ_{LF} and (γ_{SF}- γ_{SL}). The decrease in γ_{LF} was exclusively responsible for improved solderability with increased test temperature because (γ_{SF}- γ_{SL}) also decreased with temperature, a trend that would cause an increase of θ_C. The drop in the value (γ_{SF}- γ_{SL}) with increased temperature was not likely the result of increased Cd/Ni oxidation as was hypothesized for the Amphenol plated samples because the R flux did not exhibit the same behavior, which would be expected from the latter's due to its reduced strength and, therefore, increased sensitivity to surface degradation.

The Erie Plating Cd/Ni finish exhibited better solderability with the RMA flux than was recorded with R flux. The better performance of the RMA flux at 230ºC was due to a higher value of (γ_{SF}- γ_{SL}) versus that of the R flux. At 245ºC and 260ºC, lower values of γ_{LF} were responsible for the RMA flux having greater solderability at these test temperatures.

A comparison was made of the solderability parameters [θ_C, γ_{LF}, and (γ_{SF}- γ_{SL})] calculated for the two Cd/Ni coating types (Amphenol and Erie Plating). It was clear from the trends discussed above, as well as from a direct comparison of the data listed in Table 2, that there was very little similarity in the solderability behavior – that is, flux type and temperature dependencies as well as actual parameter magnitudes – between the Amphenol and Erie Plating, Cd/Ni coatings. In conclusion, if the solderability metric were based just on the contact angle θ_C, the Erie Plating Cd/Ni coatings exhibited generally better solderability than did the Amphenol coatings.

3.2 Contact Angle Test Data: Zn-Ni Plated 304L Stainless Steel

The Zn/Ni plated samples were provided by the Erie Plating Company. Non-wetting resulted from all tests regardless of solder flux or test temperature. A sample of a wetting balance plot generated by the use of an RMA flux and test performed at 260 ºC is shown in Figure 10. The solder meniscus was never formed. In fact, the trace did not reach the zero point. Non-wetting was similarly observed with the meniscometer tests. These tests were reflected in Table 2 by NW (non-wetting). The poor solderability could be related to the cracked morphology of the zinc layer and requires further study.

3.3 Wetting Rate (W_R) and Wetting Time (TF_{max}) Test Results

An analysis was also performed on the wetting rate: W_R, and the wetting time, TF_{max}. In the case of the Amphenol Cd/Ni plated samples, both fluxes exhibited the expected increase in wetting rate (Figures 11-12) and concurrently, decrease in wetting time (Figures 13-14), as the test temperature was increased. The magnitude of these trends was similar between the two fluxes. As expected, the RMA flux resulted in significantly

faster wetting rate than was observed with the R flux. Similarly, the wetting times were shorter with the RMA flux. This trend is typical for nickel surface finishes.

Analyses of wetting rate (Figures 11-12) and wetting time (Figures 13-14) were also performed on the Erie Plating Cd/Ni coatings. The values of the wetting rate were significantly less than those observed with the Amphenol coatings. This could be a result of the solder dissolving all of the nickel plating and wetting the underlying stainless steel. Typically stainless steel does not wet as readily as nickel. The wetting rate increased with test temperature in the case of both the R and RMA flux types. The wetting time was equal to the entire test duration for all flux and temperature combinations with the exception of the RMA flux used at 260ºC. As such, this parameter was considerably longer than the wetting times recorded on Amphenol coatings. In summary, the wetting rate and wetting time performance of 63Sn-37Pb solder was better on the Amphenol Cd/Ni coating and more so, with the RMA flux. The difference was of considerably lesser magnitude for the R flux. Converse to the contact angle data, the wetting rate and wetting time data suggests that the Amphenol coatings have better solderability than the Erie Plating Cd/Ni coatings.

4. Summary

Cadmium plating is the preferred method for providing corrosion protection and solderability of the stainless steel shell on the MC4636 lightning arrestor connector (LAC) to be used on the W76-1 system. This study considered the use of Zn as an environmentally friendly replacement for cadmium in this application. The solderability of Cd/Ni-plated and Zn/Ni-plated stainless steel samples was studied using the wetting balance and the meniscometer test methods. Tests were performed with an R and RMA

flux and test temperatures of 230ºC, 245ºC, and 260ºC. Contact angle, $\theta_{C,}$ served as the generalized solderability metric. The wetting rate and wetting time parameters were also collected.

The solderability of the Erie Plating Cd/Ni coatings was better than that of similar Amphenol coatings. Although the θ_C data indicated that both Cd/Ni platings would provide adequate solderability, the wetting rate and wetting force data showed the Amphenol coatings to have better performance. The Zn/Ni coatings exhibited non-wetting under all flux and temperature conditions, although cracks in the Zn surface layer could degrade solderability under the test conditions.

References

1. Edwin P. Lopez, Paul T. Vianco, and Jerome Rejent, "Solerability Testing of 95.5Sn-3.9Ag-0.6Cu Solder on Oxygen-Free High Conductivity Copper and Au-Ni-Plated Kovar", Journal of Electronic Materials, Vol. 32, No. 04, 2003, Pg. 254-260.
2. P. Vianco, "An Overview of the Meniscometer/Wetting Balance Techniques for Wettability Measurements". The Metal Science of Joining, eds. By M. Cieslak, etal (TMS, Warrendale, PA: 1992) pp. 265-284.
3. R. J. Klein Wassink, Soldering in Electronics (Ayr, Scotland: Electrochemical Publications Limited, 1984), p. 235.

Table 1 - "Relative Wettability Guideline" Using Contact Angle (θ_C) As "General" Metric

Contact Angle (θ_C) Range	Relative Wettability
$0^o < 0 < 10^o$	Perfect
$10^o < 0 < 20^o$	Excellent
$20^o < 0 < 30^o$	Very Good
$30^o < 0 < 40^o$	Good
$40^o < 0 < 50^o$	Adequate
$55^o < 0 < 70^o$	Poor

Table 2 - Solderability Parameters of Contact Angle (θ_C), Solder Flux Interfacial Tension (γ_{LF}), Wetting Rate (W_R) and Time to Maximum Wetting Force (TF_{max}) for Cd/Ni and Zn/Ni plated Stainless Steel

Substrate Material	Solder Alloy	T °C	Flux	θ_C °	γ_{LF} (dyne/cm)	W_R (mN/sec)	TF_{max} (sec)
Cd-plated Stainless Amphenol	63Sn-37Pb	230	RMA R	35.6 ±4.1 19.1 ±5.9	466.3 ±28.5 345.6 ±28.8	15.3 4.9	4.2 10.0
		245	RMA R	39.4 ±6.0 31.8 ±3.5	489.3 ±44.2 349.2 ±27.0	22.0 6.4	2.5 7.1
		260	RMA R	33.1 ±4.6 30.0 ±8.5	428.6 ±30.3 310.5 ±51.1	24.0 10.7	2.2 6.9
Cd-plated Stainless Erie	63Sn-37Pb	230	RMA R	31.1 ±5.7 43.1 ±8.3	428.9 ±36.9 418.4 ±92.1	3.8 2.2	19.9 19.9
		245	RMA R	21.5 ±6.6 38.9 ±7.5	368.3 ±35.1 442.3 ±63.4	6.8 3.2	19.7 20.0
		260	RMA R	20.0 ±9.6 26.5 ±12.5	312.2 ±45.2 362.0 ±73.0	9.1 4.7	11.0 19.4
Zn-plated SS-Erie		230	RMA R	NW NW	NW NW	NW NW	NW NW
		245	RMA R	NW NW	NW NW	NW NW	NW NW
		260	RMA R	NW NW	NW NW	NW NW	NW NW

NW = Non-Wetting
RMA = Rosin Mildly Activated
R = Rosin

Figure 1 – Equilibrium Balance of Three Interfacial Tensions (γ_{SF}, γ_{SL}, and γ_{LF})

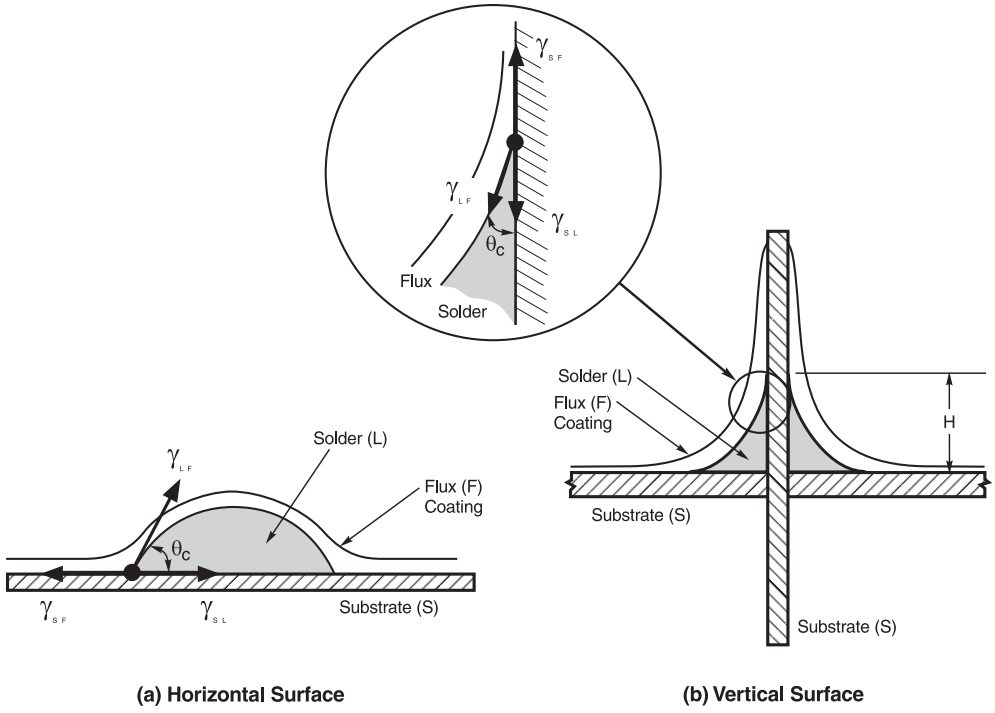

Figure 2 – Test Configuration for the Meniscometer and Wetting Balance Techniques

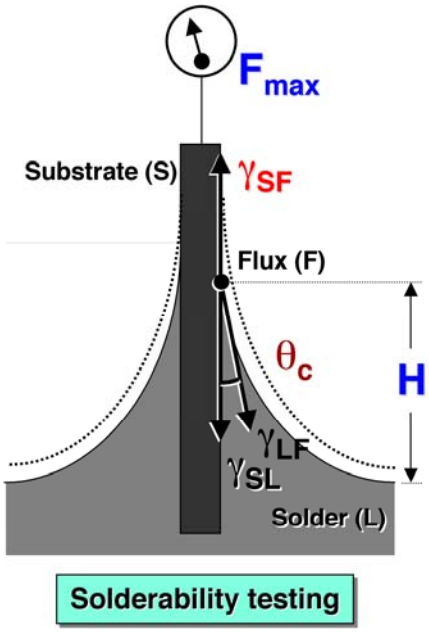

Figure 3 - Wetting Balance Data Representing The Development of the Solder Meniscus With Time

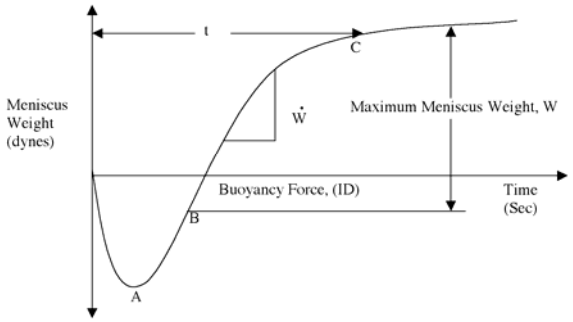

Figure 4 – SEM Image (secondary electron, SE) of 304L Stainless Steel Plated with Ni solderable layer and Cd protective layer by Amphenol.

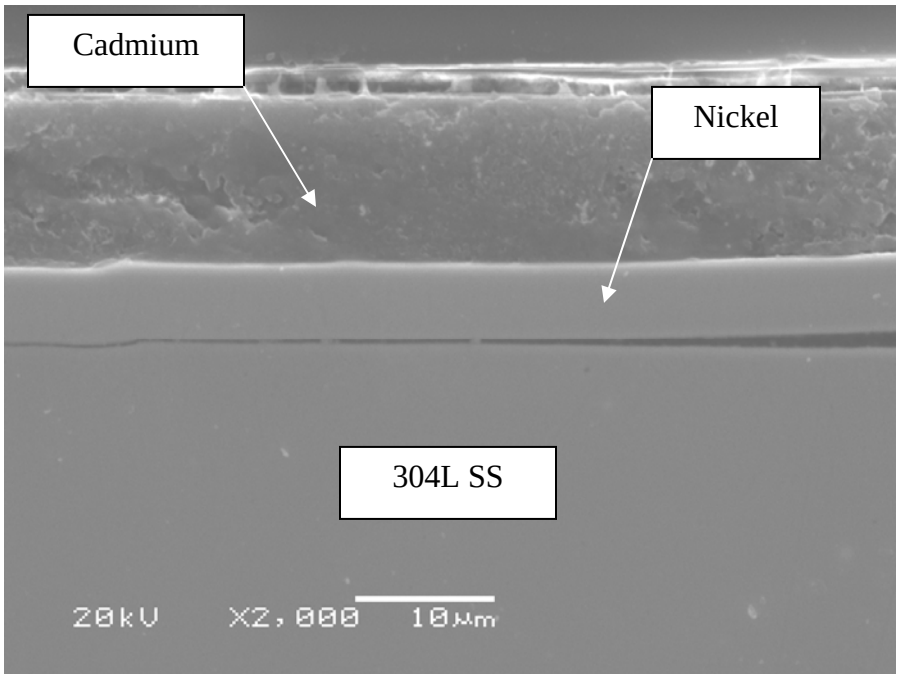

Figure 5 – SEM Image (backscatter electron, BSE) of 304L Stainless Steel electroplated with Ni solderable layer and Cd protective layer by Erie Plating.

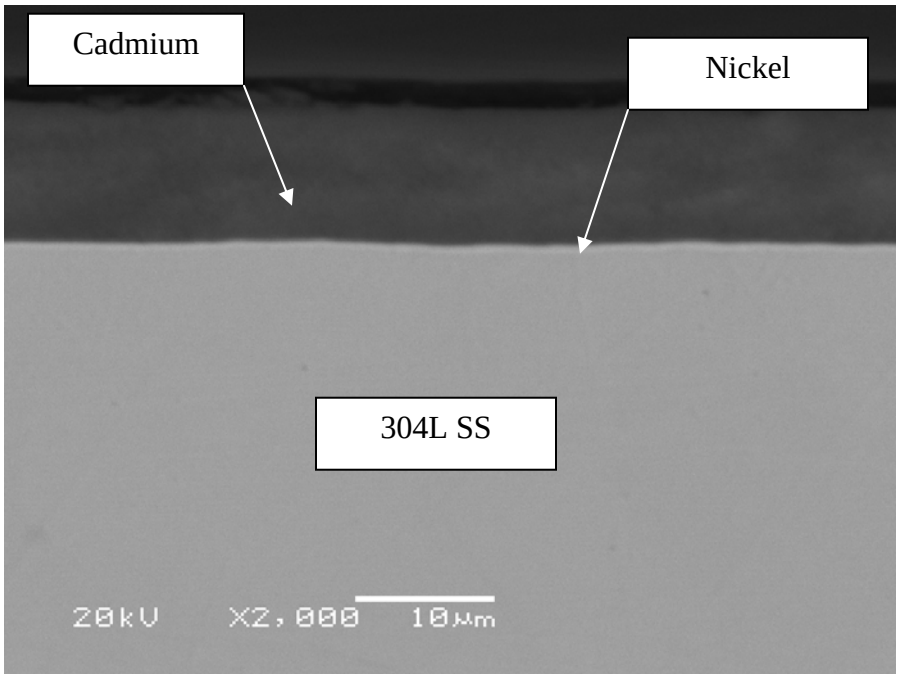

Figure 6 - Erie Plate BES Image of 304L Stainless Steel Plated With Nickel Under Layer and Zinc Top Layer

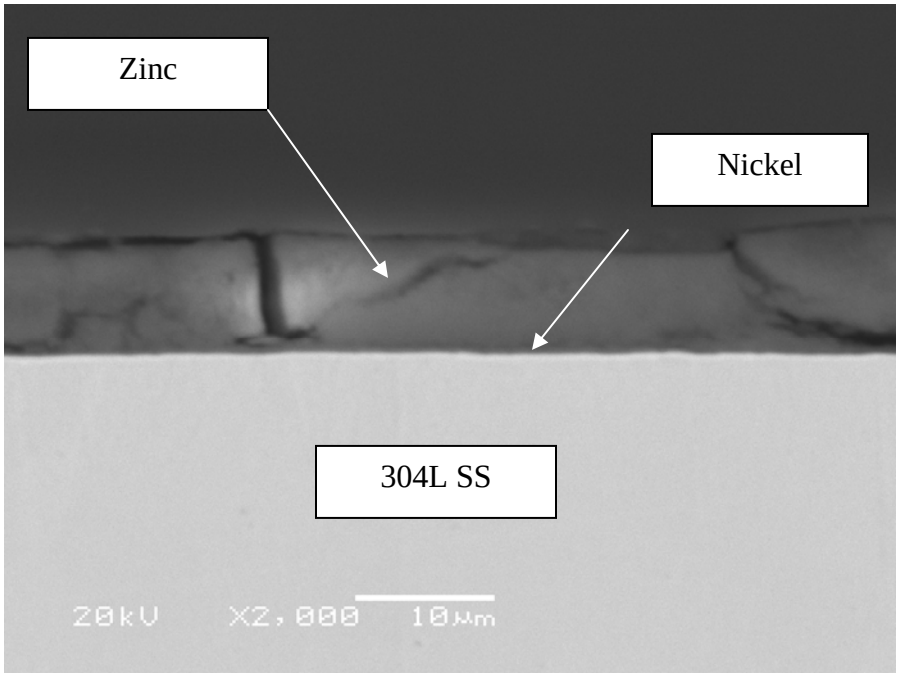

Figure 7 – EDS Spectral Imaging - reaction area at the solder front of coupon (Amphenol) 200 um field of view.

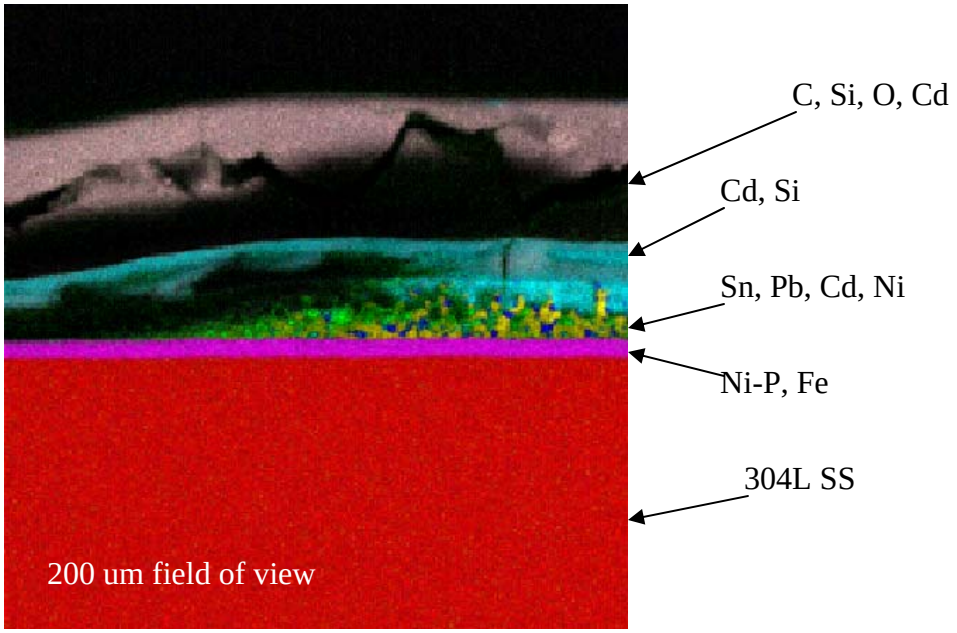

Red = Substrate (Fe, Cr, Ni)
Green = Si, Sn, Cd, Pb, Ni
Blue = Pb, Sn
Cyan = Cd, Si
Magenta = Ni, P, Fe
Yellow = Sn, Ni, Pb
White = glass (Si, O, Na, Cd)

Figure 8- Contact Angle As A Function of Temperature for R Flux On Cd-Ni Plated 304LSS

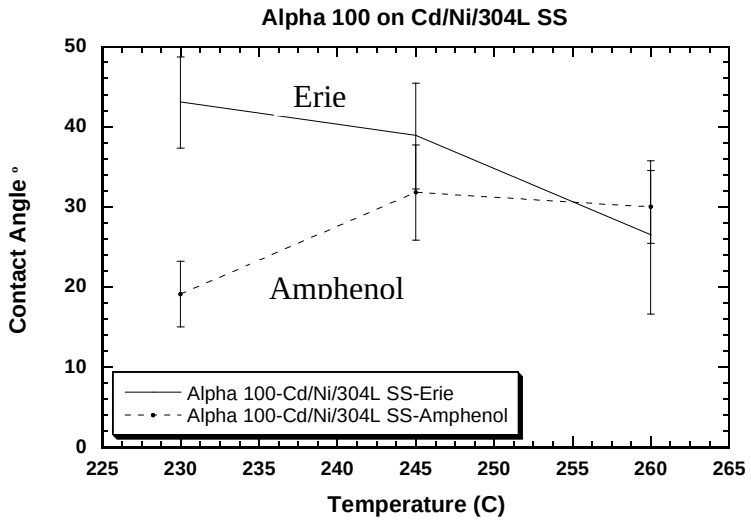

Figure 9 - Contact Angle As A Function of Temperature for RMA Flux On Cd-Ni Plated 304LSS

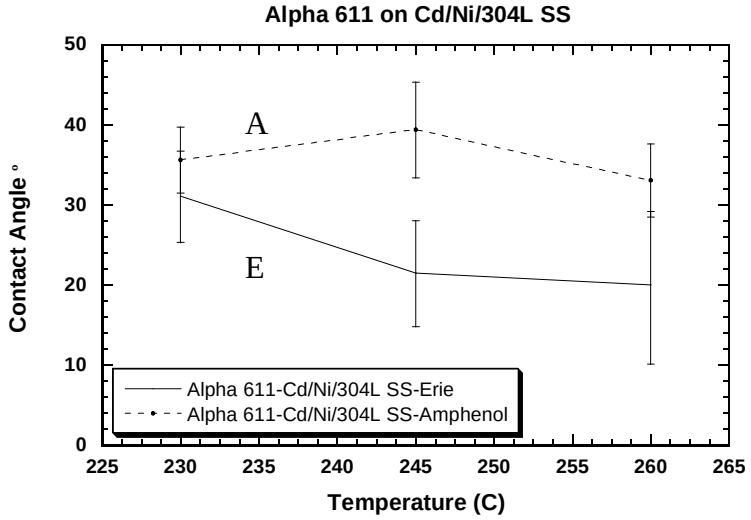

Figure 10 – Erie Plated Wetting Balance Trace For Zn-Ni Plated 304l SS at 260ºC

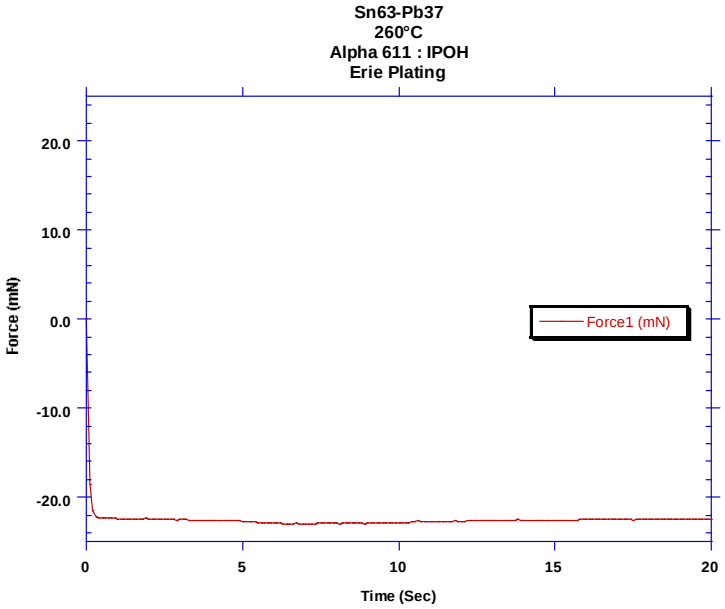

Figure 11 – Wetting Rate (W_R) As A Function of Temperature for Cd-Ni Plated 304LSS Using R Flux

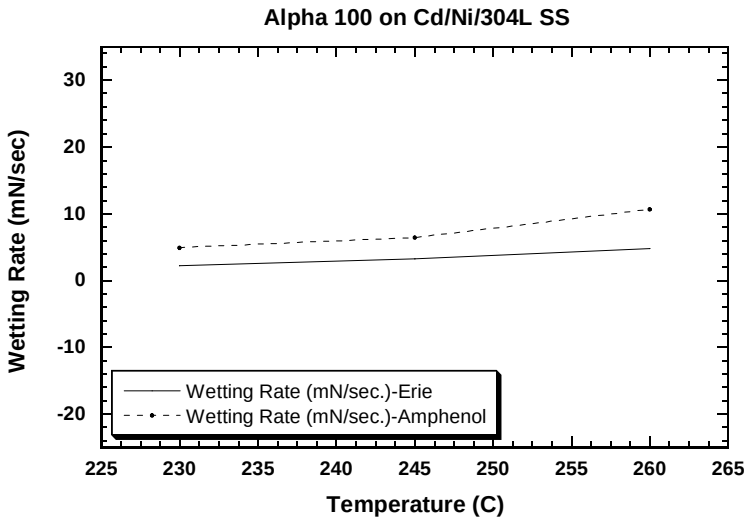

Figure 12 - Wetting Rate (W_R) As A Function of Temperature for Cd-Ni Plated 304LSS Using RMA Flux

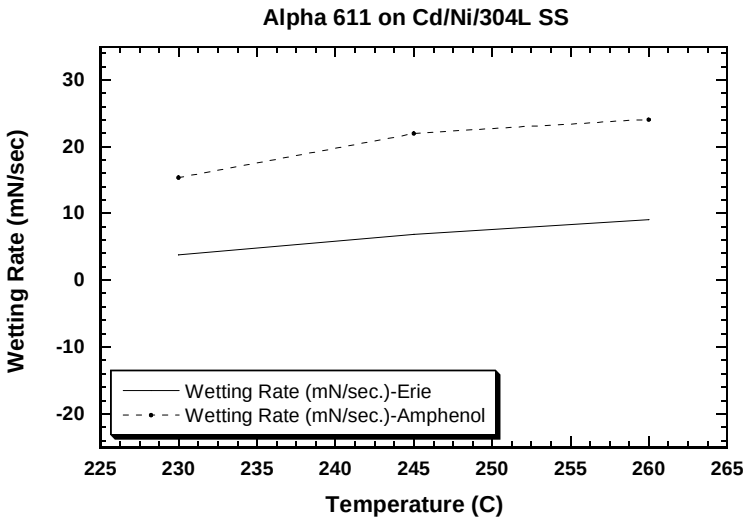

Figure 13 - Time To Maximum Force (TF_{max}) As A Function of Temperature Using R Flux

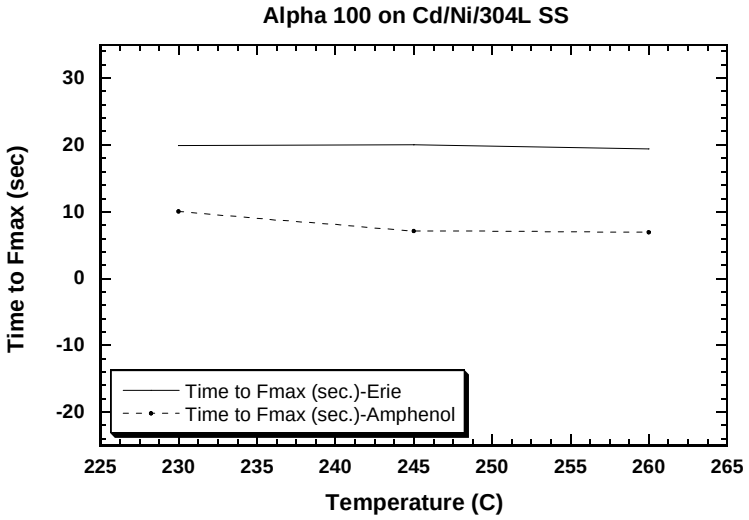

Figure 14 - Time To Maximum Force (TF_{max}) As A Function of Temperature Using RMA Flux

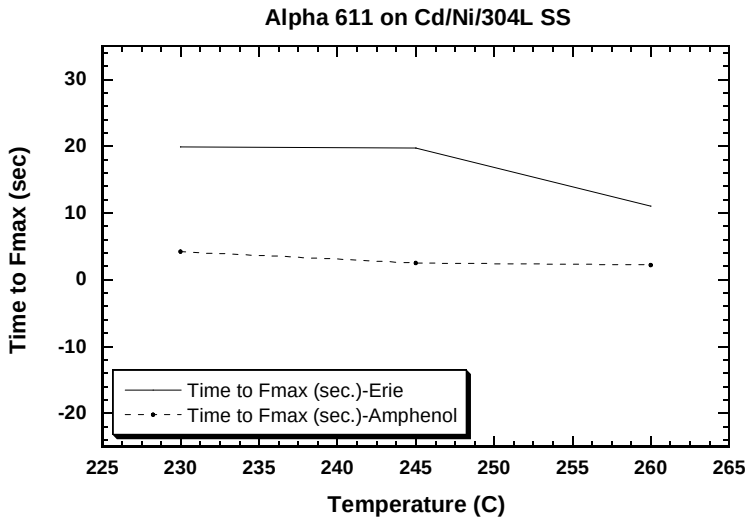

6. Distribution List

Sandia National Laboratories

Copies	Mail Stop	Dept.	
1	0523	1733	L. A. Andrews
1	0523	1733	J. E. Christensen
1	0523	1733	T. L. Ernest
1	0523	1733	J. O. Harris
1	0523	1733	D. L. South
3	0888	1832	E. P. Lopez
1	0888	1832	N. R. Sorensen
1	0888	1832	F. D. Wall
1	0889	1833	F. M. Hosking
1	0889	1833	M. F. Smith
1	0889	1861	P. T. Vianco
1	0889	1861	J. A. Rejent
1	0889	1861	J. J. Martin
1	0889	1861	J. W. Braithwaite
1	0481	2132	D. R. Helmich
1	0481	2132	M. A. Rosenthal
1	0481	2132	S. E. Slezak
1	0481	2132	H. D. Radloff
1	0481	2132	J. E. Riggs
1	0523	1733	D. R. Salmi
1	0523	1733	W. D. Cain
1	9034	8221	R. A. Van Cleave
1	9018	8940-2	Central Technical Files
2	0899	4916	Technical Library
1	0612	4912	Review & Approval Desk For DOE/OSTI

Honeywell FM&T KCP

1	2B37	462	J. M. Emmons
1	2B37	462	S. Halter
1	2B37	462	R. Taylor
1	2D39	EE3	D. Ferguson
1	2D39	EE3	D. Prigel